

Spent Media Analysis with an Integrated CE-MS Analyzer of Chinese Hamster Ovary Cells Grown in an Ammonia-Stressed Parallel Microbioreactor Platform

By Kathryn Elliott, Ji Young L. Anderson, Colin M. Gavin, Kenion H. Blakeman, Sarah W. Harcum, and Glenn A. Harris

Abstract

When working on biotherapeutic process development, the analysis of spent cell culture media is often a daily practice during the optimization of bioreactor conditions and media composition. The introduction of parallel microbioreactor systems has decreased the complexity and costs of process development by allowing for concurrent studies of multiple bioreactor and media variables. However, the bioreactors' small volumes (typically less than 250 mL) limit the volume of media one can extract for daily sampling. We describe a means to analyze spent media with an integrated microchip capillary electrophoresis mass spectrometer (CE-MS) analyzer with minimal sample volume requirements and rapid analysis time. The platform was evaluated with a parallel microbioreactor system (ambr[®] 250) culturing a Chinese hamster ovary (CHO) cell line stressed by varying levels of ammonia (NH₃).

The spent media analysis identified net increases in the levels of the amino acids (AA) Ala, Arg, Asp, Glu, Gly, His, Ile, Leu, Lys, Phe, Thr, Trp, Tyr, and Val in all bioreactors, with Gly levels showing increases in excess of 8-fold initial levels in all bioreactors. Other media components either steadily decreased in concentration or were completely depleted by the end of culture. For example, Asn was depleted in all of the unstressed and 10 mM NH₃-stressed bioreactors, but was approximately twice as high as the initial levels in the 30 mM NH₃-stressed bioreactors at the end of the culture periods. Also, the 30 mM NH₃-stressed condition may have caused either complete degradation or rapid consumption of choline, since it was no longer present starting at the $t = 36$ h sampling. Overall, the monitored media components were observed to have independent trajectories based on feeding and consumption by the cells, and depending on the stressed condition. The capability to have more frequent spent media analyses would allow for real-time observation of these process changes and associated control strategies.

1. Introduction

There have been considerable efforts expended to improve Chinese hamster ovary (CHO) productivity with media optimization and feeding strategies, but protein titers and critical quality attributes are still challenging to obtain in a timely and cost-effective way.^[1-4] The nutrient fluxes in media are an important signature of cell metabolism and have been used to better understand the metabolic state of the cells which influence titers and critical quality attributes.^[5-8] Two of the most important components of chemically defined cell culture media are amino acids (AA) and vitamins. AAs are critical for cell growth and are the building blocks of the therapeutic proteins engineered for bioprocessing. AAs in cell culture media were originally derived from serum, but fears of contamination and lot-to-lot variability shifted the emphasis towards supplementation with individual essential and nonessential AAs.^[9] Vitamins are integral to intracellular functions and metabolism but are not commonly synthesized *in vivo*. Supplementation of vitamins is common, but since many vitamins are unstable and prone to degradation, routine monitoring is encouraged.^[10]

In process development and cell culture labs, there has been a rapid adoption of automated microbioreactor systems. These systems provide faster turnaround times between processes, improved standardization between labs, and allow for low-volume parallel reactor runs. Unfortunately, there are very few online or at-line process analytical technologies capable of supporting these automated, multiplexed systems.^[11] Traditionally, enzymatic biochemical analyzers have been used to deliver basic metabolic data from bioreactors and cultures, such as the concentration of salts, glucose, lactate, and ammonia (NH₃).^[12] Recently, Raman spectroscopy has been implemented online in single bioreactors to provide "fingerprints" of chemical structure and composition of the media. However, Raman has inherent limitations with autofluorescence, absorption from turbid media, baseline drift, optical density interferences from cell concentration changes, scalability, and sterilization concerns with its probes.^[12] Chromatography-based instrumentation is often impractically complicated for upstream process development suites, so it is placed in centralized analytical labs. Running spent media analysis using chromatography^[13-16] is associated with

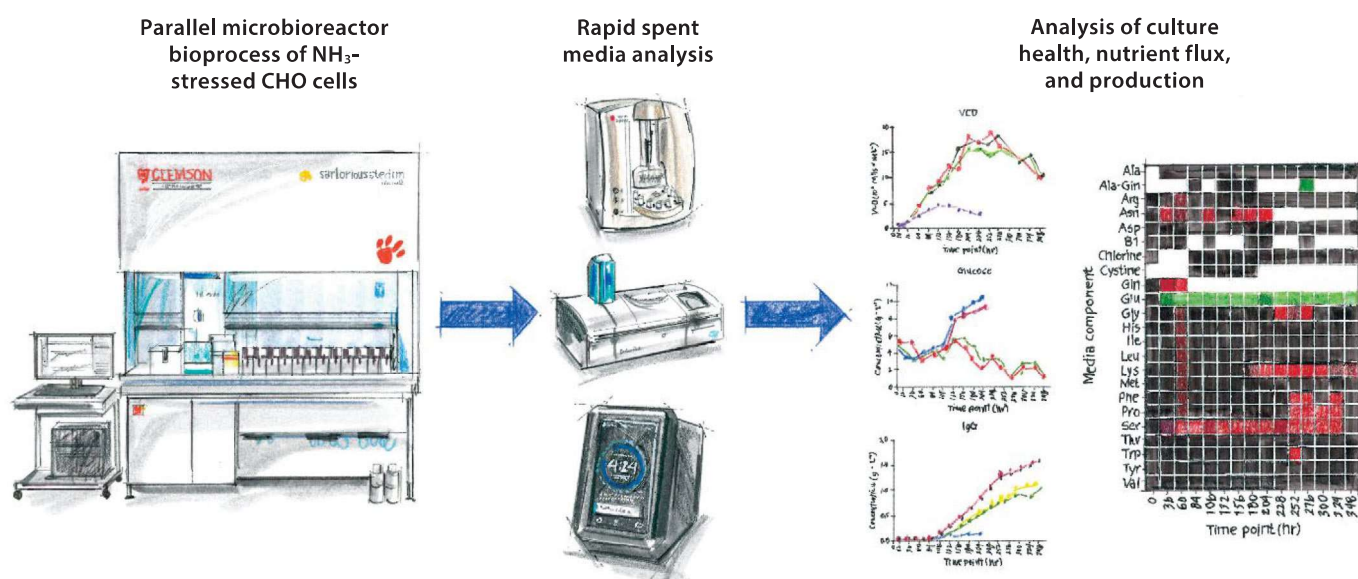


FIGURE 1. A parallel microbioreactor process of CHO cell cultures was the biological model used for demonstration. Spent media analysis was run on a new integrated benchtop CE-MS analyzer.

significant time delays from sampling and sample preparation steps including chemical derivatization. Further, the large instrument size and significant sample volume requirements are incompatible with microbioreactors and frequent sampling.

We describe an integrated microfluidic capillary electrophoresis (CE) separation coupled to a miniature ion-trap mass spectrometer (MS)^[17] configured for automated quantitation of approximately 30 components including AAs, dipeptides, and vitamins. The system requires only 10 μL of sample and seven minutes for a complete multicomponent assay, and is the size of a desktop computer tower. Operation is demonstrated on NH_3 -stressed CHO cell culture runs on a parallel microbioreactor system (**Figure 1**).

2. Material and Methods

2.1 Materials

LC-MS grade water, isopropanol, formic acid (99.5+ % purity), and ammonium acetate were purchased from Fisher Scientific (Optima grade). Choline chloride, nicotinic acid, and an AA standard mixture containing all 20 AAs (1 mM each) were obtained from Fisher Scientific. Thiamine hydrochloride, pyridoxine hydrochloride, pyridoxal hydrochloride, nicotinamide, 3,7-diaminoheptanoic acid, 5-fluorotryptophan, 3-methylaspartic acid, 2-piperazinecarboxylic acid, and L-cystine, were purchased from Sigma-Aldrich. L-alanyl L-glutamine was obtained from Alfa Aesar.

2.2 Bioprocess Conditions

A recombinant CHO-K1 (clone A11) from the Vaccine Research Center at the National Institutes of Health, which expresses the anti-HIV antibody VRC01 (IgG1), was used. The inoculum train was expanded in 250 mL shake flasks with

70 mL ActiPro media (GE Healthcare) maintained at 5% CO_2 and 37°C. The bioreactors were ambr 250 benchtop systems (Sartorius Stedim) with two pitched blade impellers and an open pipe sparger. The bioreactors were inoculated at a target cell density of 0.4×10^6 cells mL^{-1} in media and fed daily beginning on day 3 with 3% (v/v) Cell Boost 7a and 0.3% (v/v) Cell Boost 7b (GE Healthcare). Dissolved oxygen was controlled at 50% of air saturation using proportional-integral-derivative (PID) control that increased the O_2 mixture in the gas sparge to 100% and stir speed from 300 to 600 rpm. A 10% antifoaming solution (GE Healthcare) was added as needed. For the ambr 250, all gases were supplied through the open pipe sparger. Overlay air was not used. The pH was controlled via sparging CO_2 and air and base pump (NaOH). The pH setpoint was 7.0 with a 0.2 dead-band. Temperature was controlled at 37°C. The NH_3 stress was applied at 12 h post-inoculation using a 1.0 M NH_4Cl solution to increase the concentration to either 10 mM or 30 mM NH_3 . A 0.5 M NaCl stock solution was used to normalize the osmolarity and volume additions to the unstressed and 10 mM NH_3 -stressed cultures to match the 30 mM NH_3 -stressed cultures.

2.3 Standard and Sample Preparation

A quantitative calibration mixture was prepared by diluting the AA mixture, L-cystine, thiamine hydrochloride, pyridoxine hydrochloride, pyridoxal hydrochloride, nicotinamide, nicotinic acid, and L-alanyl L-glutamine to 5, 10, 25, 50, and 100 μM in 40% isopropanol. Each sample in the set had 50 μM of each internal standard (3,7-diaminoheptanoic acid, 5-fluorotryptophan, 3-methylaspartic acid, and 2-piperazinecarboxylic acid) and 0.2 M ammonium acetate. A performance qualification sample was prepared by diluting all compounds from both the calibration mixture, at 25 μM each, with the internal standards, at 50 μM each, in

40% isopropanol with 0.2 M ammonium acetate. All bioreactor samples were centrifuged at 9000 xg for 15 minutes to remove cells. The supernate was diluted 1:100 with the 40% isopropanol with 0.2 M ammonium acetate, and internal standards added at 50 μM each.

2.4 Instrumentation

Viable cell density (VCD) and viability were measured using the trypan blue exclusion method obtained using the Vi-Cell XR cell viability analyzer (Beckman Coulter). Extracellular glucose, lactate, IgG, and NH_3 concentrations were measured using a Cedex Bioanalyzer (Roche Diagnostics). The CE-MS analyzer was developed in-house. Design and fabrication of the microfluidic chip have previously been described in detail.^[18] Briefly, a 10 cm channel was used to separate the components of the media. An aqueous solution containing 40% isopropanol with approximately 5% formic acid was used for the background electrolyte (BGE). Twenty μL of prepared sample was added to the sample well and 125 μL of BGE was used to fill the other wells. Hydrodynamic injection (4 psi) was used to introduce 3.6 nL of sample to the separation channel. A separation field of 1000 $V\ cm^{-1}$ was applied to separate the analytes over four minutes. Electrospray ionization was performed on-chip at a field strength of 3500 $V\ cm^{-1}$. The miniature mass spectrometer employed a microscale stretched-length ion trap^[19,20] operating in the 0.5–1.0 torr range. The continuous flow of the atmospheric inlet to the MS was serviced with a custom multistage scroll pump (908 Devices). Ions were transported from the microfluidic chip to the ion trap through an aperture biased at +15 V. An air filter consisting of a Sunon blower fan (1 W blower fan powered at 6 V) with activated charcoal filter media (Permatron) was used to filter the air near the aperture.

A calibration curve for the CE-MS analyzer was developed using the five standard solutions at 5, 10, 25, 50, and 100 μM in 40% isopropanol (as described in section 2.3). Each of the standards were analyzed in triplicate. Between each sample, the sample well was rinsed three times with fresh BGE to minimize carryover. After the rinsings, a blank run was used to ensure there was no detectable signal from the previous sample. Each of the bioreactor samples were analyzed in triplicate. The performance qualification sample was used to ensure that analyzer performance remained consistent over time, and was run in triplicate after every sixth sample.

2.5 Data Processing

All data acquisition and processing from the CE-MS system were performed using in-house software (C++ and Python) designed to be used without operator intervention. Peaks were extracted from two-dimensional CE-MS datasets, and alignment was performed against expected migration times from earlier analyses of standards. Peaks were identified, based on migration time and mass using a modified version of the Hungarian algorithm for the linear sum assignment problem.^[21] Finally, peak area integration was performed using a non-parametric, matrix

factorization-based approach, which allowed for deconvolution of co-eluting species in the presence of non-uniform peak shapes. For quantitation, separate response curves for internal standards and analytes were constructed. For the internal standards, a linear model was used to fit peak areas as a function of injection volume. This allowed for uniform correction of the nominal analyte concentrations despite varying response factors for the internal standards. Following this correction, a non-linear calibration curve was produced for each analyte, as the combined CE and mass spectral response tends to be nonlinear over the full dynamic range of the system. The calibration curves were used to compute estimated concentrations and associated standard errors for the analytes of interest in the bioreactor samples. Averaged concentrations of the CE-MS runs were normalized to the first detected day of each detected component for the bioreactors. For most components, that was at the first sample point ($t=0$ h). However, for Ala it was at the second sample point ($t=36$ h). Graphpad Prism (v8.1.2) software was used for data visualization.

3. Results and Discussion

Cell culture health is often monitored using several attributes of the cell population and general indicators of metabolism. The viability of cell populations unstressed and minimally stressed by NH_3 (0–10 mM) showed very minimal deviation. There was an increase in VCD through the initial 180 h of growth, followed by a plateau of VCD through $t=252$ h (**Figure 2A**). The final 96 h of the process exhibited a loss of viability. The same overall trend was observed in the 30 mM NH_3 -stressed bioreactors, but at a more accelerated rate. The VCD increased slowly through $t=108$ h of culture, plateaued through $t=156$ h, and then decreased at $t=204$ h when the process was stopped. Despite the changes in VCD among all the treatments, the cell viability was similar through $t=132$ h (**Figure 2B**). After this, the 30 mM NH_3 -stressed bioreactors experienced a sudden loss in viability over the subsequent 72 h. In contrast, the unstressed and 10 mM NH_3 -stressed bioreactors only experienced a decrease of cell viability at approximately $t=228$ h, with a uniform decline across all four bioreactors.

NH_3 (**Figure 2C**), lactate (**Figure 2D**), and glucose (**Figure 2E**) profiles from the bioreactors exhibited similar profiles with significant deviations only in the 30 mM NH_3 -stressed bioreactors. NH_3 levels gradually increased to approximately 10 mM in both unstressed bioreactors. The two 10 mM NH_3 -stressed bioreactors maintained that level throughout the process. The 30 mM NH_3 -stressed bioreactors gradually decreased from the 30 mM NH_3 -spike at $t=12$ h to approximately 20 mM at $t=204$ h. For both lactate and glucose levels, all bioreactors maintained very similar ranges until $t=108$ h. After this time, both the levels of lactate and glucose rose quickly in the 30 mM NH_3 -stressed bioreactors, which coincided with the decrease of both VCD and cell viability.

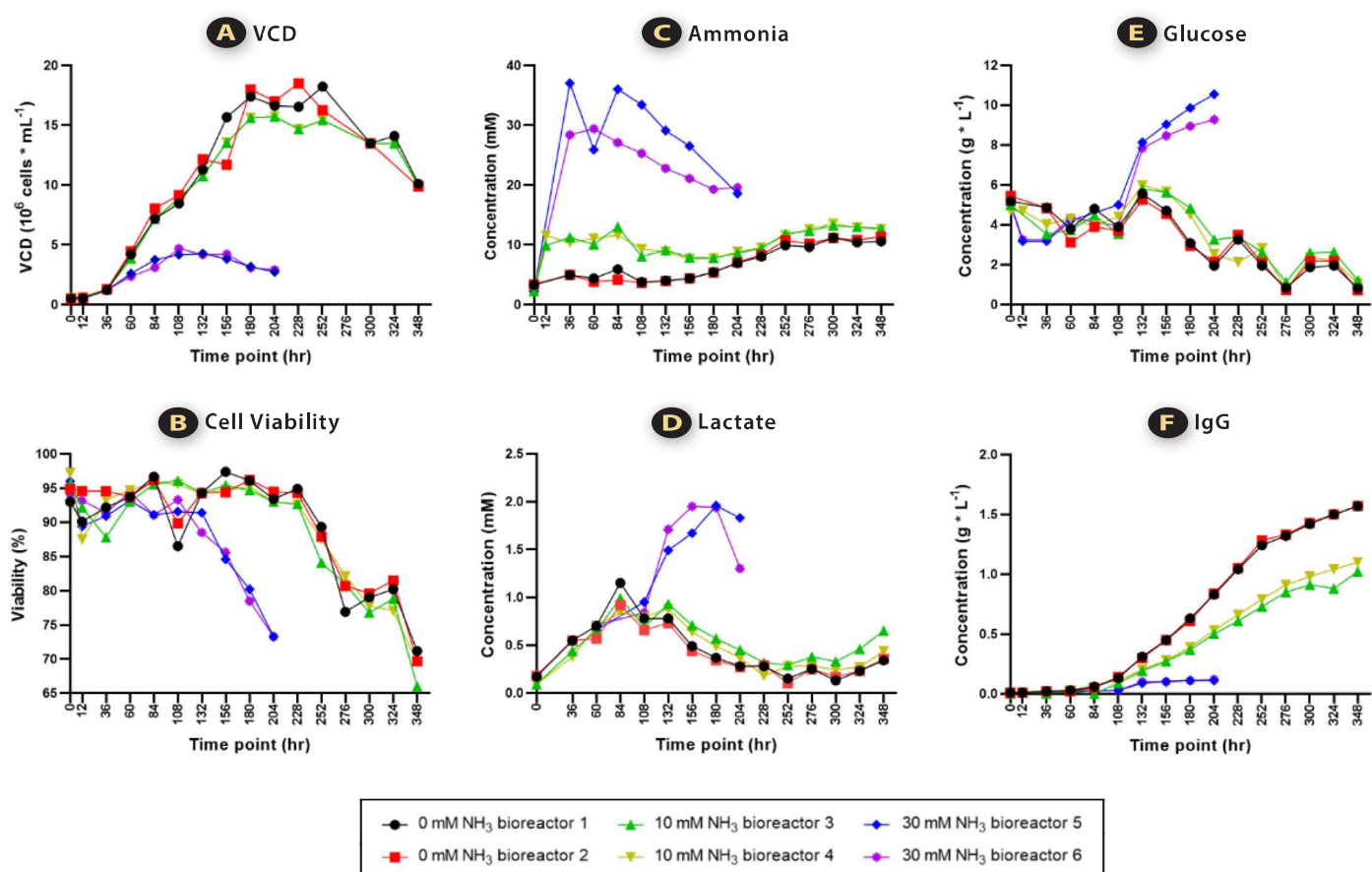


FIGURE 2. Cellular and biochemical profiles for duplicate unstressed (0 mM) and NH_3 -stressed (10 and 30 mM) bioreactors: **(A)** VCD; **(B)** cell viability; **(C)** NH_3 ; **(D)** lactate; **(E)** glucose; and **(F)** IgG protein (titer) concentrations.

Levels of IgG were the only conventional metric that exhibited varying levels between all three test conditions (**Figure 2F**). For the unstressed bioreactors, the final levels of IgG were 1.57 g L^{-1} in both bioreactors. For the 10 mM NH_3 -stressed bioreactors, there was a slower increase in IgG concentrations with a slightly higher amount of IgG produced in bioreactor 4 (1.10 g L^{-1}) compared to bioreactor 3 (1.02 g L^{-1}). Even lower amounts of IgG were measured in the 30 mM

NH_3 -stressed bioreactors. Bioreactor 5 had only 0.12 g L^{-1} IgG and bioreactor 6 had 0.11 g L^{-1} at the end of culture. For a direct comparison at $t=204 \text{ h}$, bioreactors 1, 2, 3, and 4 had measured levels of 0.83, 0.84, 0.50, and 0.53 g L^{-1} IgG, respectively.

Across all bioreactors, there was a build-up of most essential AAs throughout the process (**Table 1**). In both unstressed bioreactors, there was a relative increase in the essential AAs

TABLE 1. Relative end-of-process levels of essential AAs.

Essential AAs	Bioreactor 1 (0 mM NH_3)	Bioreactor 2 (0 mM NH_3)	Bioreactor 3 (10 mM NH_3)	Bioreactor 4 (10 mM NH_3)	Bioreactor 5 ^a (30 mM NH_3)	Bioreactor 6 ^a (30 mM NH_3)
His	1.3 ± 0.2	1.2 ± 0.1	1.7 ± 0.1	1.5 ± 0.3	2.1 ± 0.1	2.2 ± 0.1
Ile	1.2 ± 0.0	1.2 ± 0.1	1.7 ± 0.1	1.2 ± 0.1	2.2 ± 0.1	2.1 ± 0.0
Leu	1.4 ± 0.1	1.5 ± 0.1	2.0 ± 0.1	1.5 ± 0.1	2.2 ± 0.1	2.1 ± 0.0
Lys	1.7 ± 0.0	1.8 ± 0.2	2.3 ± 0.1	2.0 ± 0.1	2.7 ± 0.3	2.7 ± 0.1
Met	0.7 ± 0.0	0.8 ± 0.1	1.2 ± 0.1	0.8 ± 0.1	1.9 ± 0.1	1.6 ± 0.2
Phe	2.8 ± 0.1	2.8 ± 0.1	3.3 ± 0.1	2.6 ± 0.3	3.7 ± 0.1	3.4 ± 0.0
Thr	2.3 ± 0.1	2.4 ± 0.3	2.8 ± 0.2	2.3 ± 0.3	3.1 ± 0.1	2.8 ± 0.2
Trp	1.0 ± 0.1	1.1 ± 0.1	1.4 ± 0.2	1.2 ± 0.3	2.1 ± 0.2	2.0 ± 0.2
Val	2.2 ± 0.0	2.2 ± 0.1	2.8 ± 0.2	1.9 ± 0.2	3.4 ± 0.1	3.3 ± 0.1

^aProcess concluded at 204 h

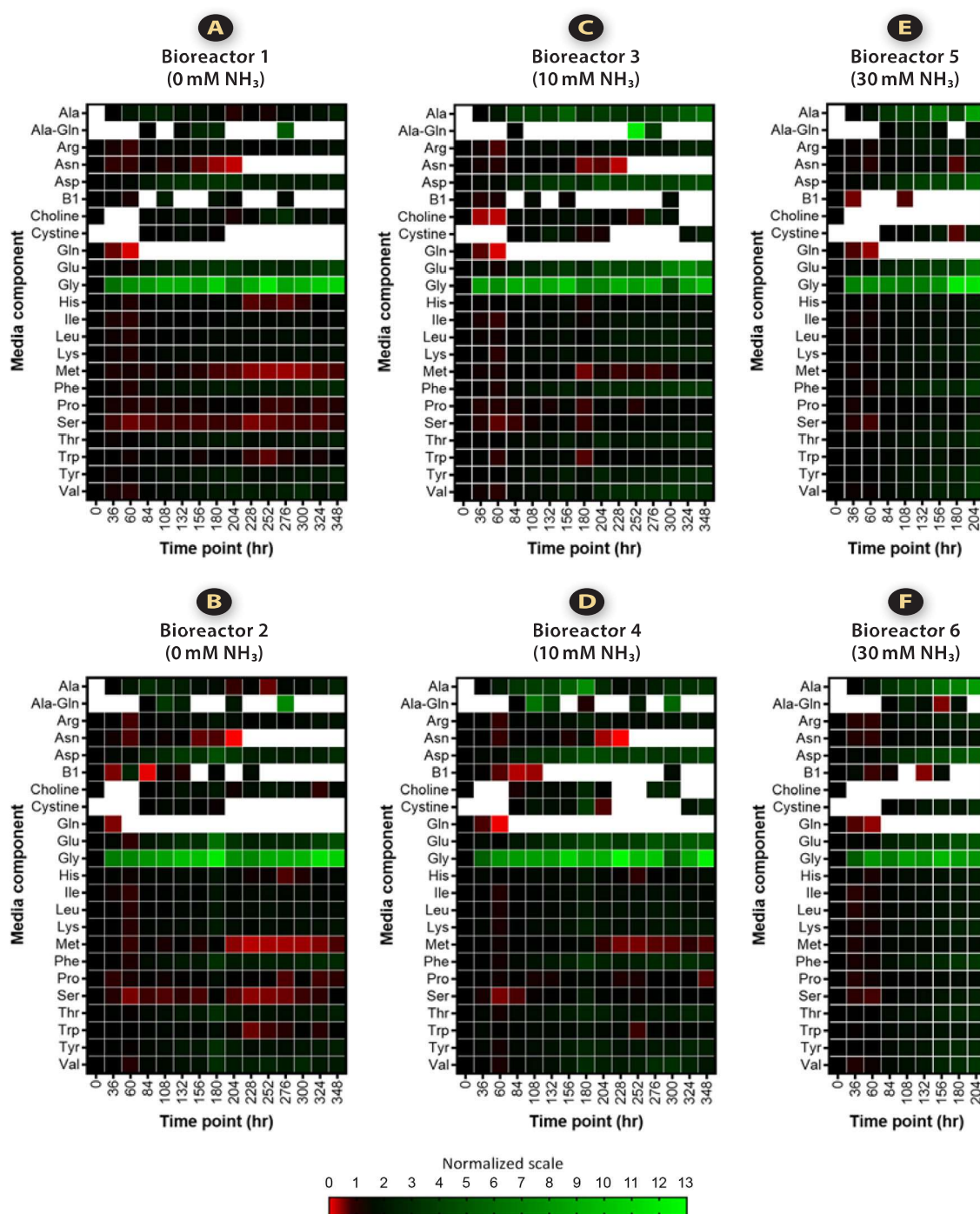


FIGURE 3. Normalized spent media analyte concentrations from the two unstressed bioreactors and the four NH₃-stressed bioreactors. Normalized values are relative to the first time point of detection of each analyte for: (A and B) 0 mM; (C and D) 10 mM; and (E and F) 30 mM NH₃-stressed bioreactors.

of His, Ile, Leu, Lys, Phe, Thr, and Val (**Figures 3A and B**). The essential AA Met decreased in relative concentration levels while Trp was relatively unchanged throughout the process. For the 10 mM NH₃-stressed cultures (bioreactors 3 and 4), the same overall trend of a net increase in essential AAs was observed. His, Ile, Leu, Lys, Met, Phe, Thr, Trp, and Val all increased their relative levels (**Figures 3C and D**). All essential

AAs increased in the 30 mM NH₃-stressed bioreactors despite ending the cultures 144 h before the other bioreactors due to cell viabilities below 70% (**Figures 2A and B**). In bioreactors 5 and 6, there were relative increases in the levels of His, Ile, Leu, Lys, Met, Phe, Thr, Trp, and Val (**Figures 3E and F**). The overall higher increase in essential AAs across all four bioreactors used in the NH₃-stressed cultures suggests that the metabolic

TABLE 2. Relative end-of-process levels of nonessential AAs.

Nonessential AAs	Bioreactor 1 (0 mM NH ₃)	Bioreactor 2 (0 mM NH ₃)	Bioreactor 3 (10 mM NH ₃)	Bioreactor 4 (10 mM NH ₃)	Bioreactor 5 ^a (30 mM NH ₃)	Bioreactor 6 ^a (30 mM NH ₃)
Ala	2.4×±0.2	2.6×±0.3	6.2×±0.2	3.3×±0.4	8.5×±0.3	8.2×±0.1
Arg	1.8×±0.2	1.9×±0.2	2.7×±0.2	1.9×±0.2	3.0×±0.1	3.0×±0.2
Asn	0.3×±0.1 ^b	0.2×±0.0 ^b	0.3×±0.0 ^c	0.2×±0.0 ^c	2.0×±0.1	1.8×±0.0
Asp	2.5×±0.1	3.0×±0.2	4.6×±0.1	4.0×±0.3	5.7×±0.2	5.4×±0.1
Gln	0.2×±0.0 ^d	0.6×±0.0 ^e	0.2×±0.1 ^d	0.3×±0.1 ^d	0.4×±0.0 ^d	0.4×±0.1 ^d
Glu	4.2×±0.2	4.6×±0.2	6.2×±1.1	5.1×±0.5	6.8×±0.0	4.7×±1.1
Gly	10.8×±1.7	10.7×±2.2	9.6×±0.5	12.4×±1.6	11.6×±3.0	7.9×±1.2
Pro	0.9×±0.0	0.9×±0.1	1.1×±0.1	0.7×±0.2	1.7×±0.1	2.2×±0.1
Ser	0.8×±0.1	1.1×±0.1	1.7×±0.1	1.1×±0.1	2.7×±0.4	2.5×±0.1
Tyr	2.3×±0.1	2.4×±0.1	2.8×±0.2	2.3×±0.2	3.1×±0.1	2.8×±0.4

^aProcess concluded at 204 h ^bDepleted by 228 h ^cDepleted by 252 h ^dDepleted by 84 h ^eDepleted by 60 h

activity of the cultures was partially inhibited, which may be correlated with the lower concentrations of IgG (**Figure 2F**).

The relative levels of the nonessential AAs (**Table 2**) were more varied than the essential AAs. Ala, Arg, Asp, Glu, Gly, and Tyr all increased in levels in bioreactors 1 and 2 (**Figures 3A and B**). Both Pro and Ser showed minor fluctuations from the initial culture conditions in bioreactors 1 and 2. Asn in bioreactors 1 and 2 was the only nonessential AA in the unstressed bioreactors to significantly decrease in concentration over the process, and was depleted by the $t = 228$ h time point. For the 10 mM NH₃-stressed bioreactors, Ala, Arg, Asp, Glu, Gly, and Tyr all increased in relative levels in bioreactors 3 and 4 (**Figures 3C and D**). Like the two unstressed bioreactors, Pro levels did not change considerably, and Ser showed a larger relative change in bioreactor 3 while displaying a small change in bioreactor 4. Consistent with the unstressed bioreactors, stressed bioreactors 3 and 4 had much lower relative levels of Asn, which were depleted by the $t = 252$ h time point. Like the levels of essential AAs, the nonessential AA levels were all higher at the end of the process ($t = 204$ h) for both 30 mM NH₃-stressed bioreactors, with relative increases for Ala, Arg, Asn, Asp, Glu, Gly, Pro, Ser, and Tyr (**Figures 3E and F**). The one nonessential AA that was present in the basal media only was Gln, as the dipeptide Ala-Gln was supplied in the feed media.

For the unstressed bioreactors, the levels of Gln were depleted by $t = 84$ h and $t = 60$ h in bioreactors 1 and 2, respectively. The initial supply of Gln was also no longer detected in the four NH₃-stressed bioreactors by $t = 84$ h.

The dipeptide Ala-Gln was periodically detected across all bioreactors starting at $t = 84$ h, since it was present in the feed (**Table 3**). This indicates that the nutrient was sometimes depleted between sampling times. Cystine was also detected starting at $t = 84$ h, as it was also a component of the feed media. Cystine was depleted in the unstressed bioreactors by the $t = 228$ h time point. This was also observed in the 10 mM NH₃-stressed bioreactors, but its levels increased, starting at the $t = 324$ time point, concluding with twice the level of cystine at the end of the process than at the initial detection point. A similar increase in the levels was observed for the 30 mM NH₃-stressed bioreactors, albeit without a window of absence, since these two bioreactors had an earlier endpoint to their processes.

Choline's levels fluctuated between the bioreactors. In the unstressed bioreactors, it was consumed completely by the second sampling point at $t = 36$ h. Its levels later increased, as it was supplemented in the feed, reaching a maximum level of $3.0 \times \pm 1.4$ in bioreactor 1 at $t = 276$ h and $2.0 \times \pm 0.5$ at $t = 252$ h in bioreactor 2. For both bioreactors, the level of

TABLE 3. Relative end-of-process levels of vitamins, dipeptides, and other nutrients.

Nutrients	Bioreactor 1 (0 mM NH ₃)	Bioreactor 2 (0 mM NH ₃)	Bioreactor 3 (10 mM NH ₃)	Bioreactor 4 (10 mM NH ₃)	Bioreactor 5 ^a (30 mM NH ₃)	Bioreactor 6 ^a (30 mM NH ₃)
Ala-Gln	5.2×±0.0 ^b	7.3×±0.0 ^b	3.8×±1.0 ^b	7.3×±0.0 ^c	1.7×±0.5	1.6×±0.0 ^d
B1	1.4×±0.0 ^b	1.5×±0.0 ^e	1.4×±0.0 ^c	1.5×±0.0 ^c	0.7×±0.0 ^f	1.6×±0.0 ^g
Choline	1.4×±0.1	1.4×±0.1	1.6×±0.9 ^c	2.7×±1.2 ^c	N/A	N/A
Cystine	1.0×±0.0 ^d	1.0×±0.0 ^d	2.5×±0.9	2.6×±0.2	2.4×±1.0	3.1×±0.7

^aProcess concluded at 204 h
^bDepleted by 300 h ^cDepleted by 324 h ^dDepleted by 204 h
^eDepleted by 252 h ^fDepleted by 132 h ^gDepleted by 180 h

choline decreased at the end of the process. In the 10 mM NH₃-stressed bioreactors, levels fluctuated but were no longer detectable after the $t = 300$ h samples. For the 30 mM NH₃-stressed bioreactors 5 and 6, there was no choline detection at any sample point after the NH₃ addition, indicating either the high concentration of NH₃ rapidly degraded the choline and/or the cells consumed the choline rapidly before the first sampling at $t = 36$ h. Since choline is integral to the formation of phospholipids, the depletion of this component from the media may be correlated to the low viable cell densities observed, beginning at the $t = 60$ h samples in the 30 mM NH₃-stressed bioreactors. Thiamine hydrochloride (vitamin B1) was introduced in both the base media and the feed. B1 levels likely fluctuated across all bioreactors due to its low levels relative to the AAs in the media. For the

unstressed bioreactors 1 and 2, the last detected levels of B1 were at $t = 276$ h and at $t = 228$ h, respectively. For the 10 mM NH₃-stressed bioreactors 3 and 4, the last detected levels of B1 were both at $t = 300$ h. For the 30 mM NH₃-stressed bioreactors 5 and 6, the last detected levels of B1 were at $t = 108$ h and at $t = 156$ h, respectively.

This analysis demonstrated that the levels of the essential and nonessential AAs, along with other nutrients, changed independently, and in some cases, suddenly, allowing real-time observation of process changes. The capability to have more frequent spent media analyses would allow for real-time observation of these process changes, such that intervention measures could be implemented. More frequent spent media analyses may elucidate the mechanisms behind these changes and improve process development timelines.

4. Conclusion

Spent media analyses were performed using an integrated CE-MS analyzer to track levels of AAs, dipeptides, and vitamins across six microbioreactors subjected to varying levels of NH₃ stress. Traditional analytic approaches were not capable of discerning significant changes between the cultures, especially early in the processes, despite dramatic differences in the measured titer. Approximately 1.4 times more IgG was produced in the unstressed systems as compared to the 10 mM NH₃-stressed bioreactors, and 13 times more IgG was produced in the unstressed systems as compared to the 30 mM NH₃-stressed bioreactors. VCDs, cell viability, lactate, and glucose values between the unstressed and 10 mM NH₃-stressed bioreactors were very

similar throughout the process. There were more pronounced changes in cell viability, lactate, and glucose levels for the 30 mM NH₃-stressed bioreactors after approximately 132 h into the process.

The data presented here demonstrated that the levels of the essential and nonessential AAs changed independently and earlier in the process. Due to NH₃ stress, AA flux changes were more sensitive than the standard metabolite panel alone. In order to better understand the mechanisms behind these AA flux changes and their relationship to protein production, more frequent sampling is needed. In the future, real-time observation of AA changes will allow for in-line process control and process optimization.

References

- [1] Ehret J, Zimmermann M, Eichhorn T, Zimmer A. Impact of cell culture media additives on IgG glycosylation produced in Chinese hamster ovary cells. *Biotechnol Bioeng*, 2019; 116(4): 816–30. <https://doi.org/10.1002/bit.26904>
- [2] Li F, Vijayasankaran N, Shen A, Kiss R, Amanullah A. Cell culture processes for monoclonal antibody production. *mAbs*, 2010; 2(5): 466–79. <https://doi.org/10.4161/mabs.2.5.12720>
- [3] Reinhart D, Damjanovic L, Kaisermayer C, Kunert R. Benchmarking of commercially available CHO cell culture media for antibody production. *Appl Microbiol Biotechnol*, 2015; 99: 4645–57. <https://doi.org/10.1007/s00253-015-6514-4>
- [4] Kyriakopoulos S, Polizzi KM, Kontoravdi C. Comparative analysis of amino acid metabolism and transport in CHO variants with different levels of productivity. *J Biotechnol*, 2013; 168(4): 543–51. <https://doi.org/10.1016/j.jbiotec.2013.09.007>
- [5] Jordan M, Voisard D, Berthoud A, Tercier L, Kleuser B, Baer G, Broly H. Cell culture medium improvement by rigorous shuffling of components using media blending. *Cytotechnology*, 2013; 65: 31–40. <https://doi.org/10.1007/s10616-012-9462-1>
- [6] Torkashvand F, Vaziri B, Maleknia S, Heydari A, Vossoughi M, Davami F, Mahboudi F. Designed amino acid feed in improvement of production and quality targets of a therapeutic monoclonal antibody. *PLoS ONE*, 2015; 10(10): e0140597. <https://doi.org/10.1371/journal.pone.0140597>
- [7] Kishishita S, Katayama S, Kodaira K, Takagi Y, Matsuda H, Okamoto H, Takuma S, Hirashima C, Aoyagi H. Optimization of chemically defined feed media for monoclonal antibody production in Chinese hamster ovary cells. *J Biosci Bioeng*, 2015; 120(1): 78–84. <https://doi.org/10.1016/j.jbiosc.2014.11.022>
- [8] Carrillo-Cocom LM, Genel-Rey T, Araíz-Hernández D, López-Pacheco F, López-Meza J, Rocha-Pizaña MR, Ramírez-Medrano A, Alvarez MM. Amino acid consumption in naïve and recombinant CHO cell cultures: producers

- of a monoclonal antibody. *Cytotechnology*, 2015; 67: 809–20. <https://doi.org/10.1007/s10616-014-9720-5>
- [9] Salazar A, Keusgen M, von Hagen J. Amino acids in the cultivation of mammalian cells. *Amino Acids*, 2016; 48: 1161–71. <https://doi.org/10.1007/s00726-016-2181-8>
- [10] Schnellbaecher A, Binder D, Bellmaine S, Zimmer A. Vitamins in cell culture media: Stability and stabilization strategies. *Biotechnol Bioeng*, 2019; 116(6): 1537–55. <https://doi.org/10.1002/bit.26942>
- [11] Jiang M, Severson KA, Love JC, Madden H, Swann P, Zang L, Braatz RD. Opportunities and challenges of real-time release testing in biopharmaceutical manufacturing. *Biotechnol Bioeng*, 2017; 114(11): 2445–56. <https://doi.org/10.1002/bit.26383>
- [12] Esmonde-White KA, Cuellar M, Uerpmann C, Lenain B, Lewis IR. Raman spectroscopy as a process analytical technology for pharmaceutical manufacturing and bioprocessing. *Anal Bioanal Chem*, 2017; 409(3): 637–49. <https://doi.org/10.1007/s00216-016-9824-1>
- [13] Mohamad-Saberi SE, Hashim YZHY, Mel M, Amid A, Ahmad-Raus R, Packeer-Mohamed V. Metabolomics profiling of extracellular metabolites in CHO-K1 cells cultured in different types of growth media. *Cytotechnology*, 2013; 65(4): 577–86. <https://doi.org/10.1007/s10616-012-9508-4>
- [14] Qiu J, Chan PK, Bondarenko PV. Monitoring utilizations of amino acids and vitamins in culture media and Chinese hamster ovary cells by liquid chromatography tandem mass spectrometry. *J Pharm Biomed Anal*, 2016; 117: 163–72. <https://doi.org/10.1016/j.jpba.2015.08.036>
- [15] Floris P, McGillicuddy N, Albrecht S, Morrissey B, Kaisermayer C, Lindeberg A, Bones J. Untargeted LC-MS/MS profiling of cell culture media formulations for evaluation of high temperature short time treatment effects. *Anal Chem*, 2017; 89(18): 9953–60. <https://doi.org/10.1021/acs.analchem.7b02290>
- [16] Chen P, Harcum SW. Effects of amino acid additions on ammonium stressed CHO cells. *J Biotechnol*, 2005; 117(3): 277–86. <https://doi.org/10.1016/j.jbiotec.2005.02.003>
- [17] Gilliland WM, Ramsey JM. Development of a microchip CE-HPMS platform for cell growth monitoring. *Anal Chem*, 2018; 90(21): 13000–6. <https://doi.org/10.1021/acs.analchem.8b03708>
- [18] Batz NG, Mellors JS, Alarie JP, Ramsey JM. Chemical vapor deposition of aminopropyl silanes in microfluidic channels for highly efficient microchip capillary electrophoresis-electrospray ionization-mass spectrometry. *Anal Chem*, 2014; 86(7): 3493–500. <https://doi.org/10.1021/ac404106u>
- [19] *Miniature charged particle trap with elongated trapping region for mass spectrometry*. Patents US8878127B2 <https://patents.google.com/patent/US8878127B2/en> and US9252005B2 <https://patents.google.com/patent/US9252005B2/en>
- [20] Blakeman KH, Wolfe DW, Cavanaugh CA, Ramsey JM. High pressure mass spectrometry: The generation of mass spectra at operating pressures exceeding 1 torr in a microscale cylindrical ion trap. *Anal Chem*, 2016; 88(10): 5378–84. <https://doi.org/10.1021/acs.analchem.6b00706>
- [21] Munkres J. Algorithms for the assignment and transportation problems. *J Soc Ind Appl Math*, 1957; 5(1): 32–8. <https://doi.org/10.1137/0105003>

Funding

Clemson University would like to acknowledge the support from the National Science Foundation (NSF) under Grant No. OIA-1736123. Any opinions, findings, and conclusions or recommendations expressed in this material are those of the author(s) and do not necessarily reflect the views of the NSF.

Disclosure of Interest

908 Devices provided travel funds and support for SWH to attend a symposium and discuss manuscript development.

Acknowledgements

We would like to acknowledge Drew Blouch, Steve Araiza, and Christopher Brown at 908 Devices Inc. for support with the CE-MS system. Both 908 Devices Inc. and Clemson University would also like to thank the National Institute for Innovation in Manufacturing Biopharmaceuticals (NIIMBL) for creating environments where groups like ours can meet and collaborate.

About the Authors

Kathryn Elliott¹, Ji Young L. Anderson², Colin M. Gavin², Kenion H. Blakeman², Sarah W. Harcum¹, **Glenn A. Harris^{2*}**

1. Clemson University, Department of Bioengineering, 105 Collings Street, Clemson, South Carolina 29634 USA

2. 908 Devices Inc., 645 Summer Street, Boston, Massachusetts 02210 USA

*Corresponding Author: gaharris@908devices.com